A dynamical study of the chemisorption of molecular hydrogen on the Cu(111) surface

1995 J. Phys.: Condens. Matter 7 7195

(http://iopscience.iop.org/0953-8984/7/36/009)

J. Phys.: Condens. Matter 7 (1995) 7195–7207. Printed in the UK

A dynamical study of the chemisorption of molecular hydrogen on the Cu(111) surface

Alessandra Forni†, Gijsbert Wiesenekker‡, Evert Jan Baerends‡ and Gian Franco Tantardini†

† Dipartimento di Chimica Fisica ed Elettrochimica, Via Golgi 19, 20133 Milano, Italy
‡ Afdeling Theoretische Chemie, Scheikundig Laboratorium der Vrije Universiteit, De Boelelaan 1083, 1081 HV Amsterdam, The Netherlands

Received 19 June 1995

Abstract. *Ab initio* band structure calculations within a density functional formalism were performed to compute the binding energy curves for atomic hydrogen interacting with high-symmetry adsorption sites of the (111) surface of copper. For a two-layer slab of Cu atoms and H coverage equal to 0.25, the binding energies are 2.23, 3.12 and 3.24 eV, for on top, bridge and threefold sites, so the chemisorption of H_2 on Cu(111) is exothermic for threefold and bridge sites, but endothermic for on top sites. Starting from the *ab initio* results for the H–Cu(111) system, a LEPS potential for the interaction of H_2 with the Cu(111) surface was built. In this model potential, the most favoured approaches correspond to a H_2 molecule parallel to the Cu surface, and have activation barriers of 0.6 eV, located at the corner between entrance and exit reaction channels. The LEPS potential was used in quasiclassical trajectory calculations to simulate the adsorption of a beam of H_2 molecules on Cu(111). The dynamical results show that (a) when H_2 is in its ground vibrational state, the dissociative adsorption probability, P_a, increases from 0 to 0.90 along a roughly sigmoidal curve when increasing the collision kinetic energy from 0.4 to 1.3 eV; (b) the vibrational energy of H_2 can be as effective as the translational one in promoting chemisorption; (c) dissociation of H_2 is inhibited by rotational motion at low j values, but enhanced by high values of j; (d) P_a scales with normal component of collision energy; (e) no azimuthal corrugation of the surface is observed.

1. Introduction

The adsorption of molecular hydrogen on copper surfaces has been the subject of many experimental [1–14] and theoretical [15–25] investigations, so that the H_2–Cu surface system has become an important model system in studies of gas–surface dynamics [26]. In particular, it has been found that the dissociative adsorption of H_2 on Cu surfaces is characterized by the presence of high activation barriers (>0.5 eV). Both translational and vibrational energy play a role in promoting chemisorption, as shown by beam experiments [2–7, 10] and theoretical calculations [15–25]. Some studies on the desorption of H_2 from Cu surfaces have elucidated the role of the H_2 rotational motion [9, 14], and the effects of the Cu surface temperature [8, 11, 14] on the process. In this paper, we present the results of a study of the dynamical aspects of the dissociative adsorption of H_2 molecules on the Cu(111) surface, using a model potential built with *ab initio* results obtained for the interaction of atomic hydrogen with the copper surface. Following a preceding work [27], where preliminary results were reported, we give here a complete, detailed and statistically more reliable analysis of the dynamics of chemisorption. In the next section, we briefly

0953-8984/95/367195+13$19.50

describe the *ab initio* band structure calculations performed in order to obtain the binding energy curves of the H atom at the most important adsorption sites of the Cu(111) surface. In the third section, we outline the procedure used to build up a model potential, based on a LEPS approach, for the interaction between molecular hydrogen and the (111) surface of copper starting from the *ab initio* results for the H–Cu(111) system. In the fourth part, the details of the classical dynamical simulations of the reactive scattering of a H_2 beam on Cu(111) are reported. In the last section, the results concerning the dissociative chemisorption probability of H_2 on the metal surface are presented and discussed, with particular emphasis on the influence of the translational, vibrational and rotational energy components of H_2 in the incident beam.

2. The H–Cu(111) interaction potential

The potential energy curve for the interaction of atomic hydrogen with the (111) surface of copper is different for different positions of the H atom on the surface, according to the periodicity and the symmetry of the fcc (111) surface. We represent the H–Cu interaction potential with a Morse function

$$V_{HCu} = D_{HCu}\{1 - \exp[\alpha_{HCu}(z^e_{HCu} - z_{HCu})]\}^2$$

where z_{HCu} is the distance of H from the (x, y) plane of the Cu(111) surface, and D_{HCu}, z^e_{HCu} and α_{HCu} are the binding energy, the equilibrium bond distance and the range parameter, respectively. The Morse parameters were assumed to be periodic functions of the (x, y) coordinates of the projection of the H atom on the (111) plane, as following

$$D_{HCu}(x, y) = D_0 + D_1\ P_1(x, y) + D_2\ P_2(x, y) + D_3\ P_3(x, y)$$
$$z^e_{HCu}(x, y) = z^e_0 + z^e_1\ P_1(x, y) + z^e_2\ P_2(x, y) + z^e_3\ P_3(x, y)$$
$$\alpha_{HCu}(x, y) = \alpha_0 + \alpha_1\ P_1(x, y) + \alpha_2\ P_2(x, y) + \alpha_3\ P_3(x, y)$$

where for $P_1\ (x, y)$, $P_2\ (x, y)$ and $P_3\ (x, y)$ the following expressions were used:

$$P_1(x, y) = \cos\omega_x + \cos\omega_y + \cos(\omega_x + \omega_y)$$
$$P_2(x, y) = (1 - \cos\ \omega_x)(1 - \cos\omega_y)[1 - \cos(\omega_x + \omega_y)]$$
$$P_3(x, y) = P_2(x, y)\sin(\omega_x + \omega_y)$$

with $\omega_x = 2\pi X/d$, $\omega_y = 2\pi Y/d$; X, Y are crystallographic coordinates ($X = 2x/\sqrt{3}$ and $Y = -x/\sqrt{3} + y$); $d = 2.55$ Å is the nearest-neighbour Cu–Cu distance in the primitive cell. The values of the parameters (D_0, D_1, D_2, D_3), $(z^e_0, z^e_1, z^e_2, z^e_3)$ and $(\alpha_0, \alpha_1, \alpha_2, \alpha_3)$ appearing in the V_{H-Cu} potential were obtained by performing *ab initio* band structure calculations on the H–Cu(111) system with the program BAND [28], which is based on a new method for density functional calculations on periodic systems. The main features of the method are: (a) a numerical integration scheme to evaluate all integrals in real space, which gives high precision and rapid convergence; (b) representation of the Coulomb potential with an expansion of the charge density in suitable function sets; (c) numerical integration over the BZ in k space through a quadratic tetrahedron method, which is accurate and quickly convergent; (d) freedom in the choice of basis functions, which allows the use of numerical atomic orbitals (Hermann–Skillman), analytic Slater-type functions and plane waves, in highly efficient basis sets for a rapid approach of the basis set limit. In the present calculations, we used the Vosko–Wilk–Nusair formulas for the exchange–correlation energy, and six k points for the on top and the threefold sites and nine k points for the bridge site in the irreducible wedge of the first BZ. After having verified the influence of the number of

layers in the Cu slab, we performed all calculations using a two-layer slab, with H coverage equal to 0.25, which ensures negligible interactions between H atoms. For the Cu atoms of the first layer we included into a frozen core all orbitals up to 3p orbitals, whereas for the Cu atoms of the second layer also the 3d orbitals were included into the core. The basis set on the first-layer Cu atoms was double-zeta 3d, double-zeta 4s and a 4p polarization function, whereas for the Cu atoms in the second layer a double-zeta 4s orbital was used. The basis set on the H atom consisted of a double-zeta 1s, a double-zeta 2s, a 2p and a 3d polarization function. For all double-zeta orbitals we used a numerical atomic orbital and a Slater-type function, except for the H 2s orbitals, for which two Slater functions were used.

Table 1. *Ab initio* binding energies, D_{HCu}, equilibrium bond distances, z^e_{HCu}, vibrational frequencies, ω_{HCu}, and Morse range parameters computed from vibrational frequencies, α_{HCu}, for atomic hydrogen interacting with high-symmetry adsorption sites of the Cu(111) surface.

	D_{HCu} (eV)	z^e_{HCu} (Å)	ω_{HCu} (cm^{-1})	α_{HCu} (Å^{-1})
On top	2.25	1.53	1770	1.59
Bridge	3.12	1.01	1237	0.945
Threefold	3.24	0.852	1078	0.428

For the H–Cu(111) system, we considered different geometries, with the H atom moving along the perpendicular (z axis) to the surface through adsorption sites of high symmetry, that is, through the on top site, the bridge site and the threefold sites. The hollow and the filled threefold sites, without and with a second-layer Cu atom underneath, respectively, were considered identical, and the parameters D_3, z^e_3 and α_3 appearing in D_{HCu}, z^e_{HCu} and α_{HCu} were set equal to zero. From the *ab initio* potential energy curves for H interacting with different Cu sites, the binding energies, equilibrium bond distances, vibration frequencies and α_{HCu} range parameters reported in table 1 were obtained. Regarding the accuracy of the Morse curves obtained in this way, we may make the following comments. First, the local density approximation employed in electronic structure calculations is known to give generally overbinding. In some cases, this overbinding is quite large such as, for instance, in the donor/acceptor bond of CO to transition metal atoms in complexes [29] and to a Cu slab [30]. For the case of the electron pair bonding of H atoms to metals, there are indications that the overbinding is much less severe, again both in complexes [29] and on metals [31]. For one H–Cu(111) distance, we have explicitly verified this by including the so-called non-local or density gradient corrections developed by Becke [32] and Perdew [33]. We obtained a reduction of the binding energy of 20%, perfectly in line with the results of [29, 31]. We have also checked the convergence with the number of layers in the slab, and we have found that increasing the slab thickness to three layers would increase the dissociation energy by less than 5%. Finally, the construction of the Morse curves entails inaccuracies of comparable magnitude, in particular, near the metal surface the Morse curves for the bridge and hollow sites give H–Cu interactions less attractive than those provided by the corresponding *ab initio* curves.

By requiring that the functions $D_{HCu}(x, y)$, $z^e_{HCu}(x, y)$, and $\alpha_{HCu}(x, y)$ appearing in the V_{HCu} potential assume in the on top, bridge and hollow sites the corresponding *ab initio* values, we obtained the following results: $D_0 = 2.91$ eV, $D_1 = -0.218$ eV, $D_2 = 0.00174$ eV; $z^e_0 = 1.14$ Å, $z^e_1 = 0.130$ Å, $z^e_2 = -0.0263$ Å; $\alpha_0 = 1.11$ Å^{-1}, $\alpha_1 = 0.162$ Å^{-1}, $\alpha_2 = -0.0164$ Å^{-1}. This V_{H-Cu} potential leads to exothermic dissociative chemisorption of H on hollow and bridge sites, with release of energy, per H atom, equal to 0.87 eV and 0.75 eV, respectively, whereas for the on top site the process is endothermic

by 0.12 eV.

3. The H_2–Cu(111) LEPS potential

For the interaction of molecular hydrogen with the copper surface, we used a modified LEPS potential [34–39], a non-pairwise potential which has correct asymptotic behaviour, appropriately describes bond breaking and formation in chemical reactions and has, in general, sufficient flexibility in the transition state region, so it can be modelled according to available experimental and theoretical information.

For a diatomic molecule, AB, impinging on a solid surface, S, the LEPS potential is

$$V_{LEPS} = Q'_{AB} + Q'_{AS} + Q'_{BS} - [J'^2_{AB} + J'^2_{AS} + J'^2_{BS} + 2J'_{AS}J'_{BS} - J'_{AB}J'_{AS} - J'_{AB}J'_{BS}]^{1/2}$$

where $Q'_i = Q_i/(1+\Delta_i)$, and $J'_i = J_i/(1+\Delta_i)$; Q_i and J_i are the Coulomb and exchange integrals of the possible diatoms i = A–B, A–S, B–S, and Δ_i are the Sato parameters, which can be used to modify the main features (saddle points, wells, etc) of the potential.

The Coulomb and exchange integrals (Q_i, J_i) of diatom i in the LEPS potential are related to the singlet and triplet states energies of the diatom: ${}^1V_i = (Q_i + J_i)/(1+\Delta_i)$ and ${}^3V_i = (Q_i - J_i)/(1-\Delta_i)$. These, in turn, are represented with Morse ${}^1V_i = D_i\{1 - \exp[\alpha_i(r_i^e - r_i)]\}^2$, and anti-Morse ${}^3V_i = D_i\{1 + \exp[\alpha_i(r_i^e - r_i)]\}^2/2$ potentials, respectively, with parameters D_i, r_i^e and α_i corresponding to binding energy, equilibrium bond distance and range parameter of diatom i. For the H–H diatom, we used the values D_{HH} = 4.75 eV, r^e_{HH} = 0.741 Å and α_{HH} = 1.97 Å^{-1}, obtained by fitting the Morse potential to *ab initio* results for the ground state of H_2 [34]. For H–Cu(111), we used the V_{HCu} potential obtained with the procedure described above. To limit the computational effort, the metal surface was assumed rigid, and no energy exchange with the incoming molecule was possible. This approximation is partially justified by the low value (6%) of the energy transfer between H and Cu atoms, when treated as hard spheres [40].

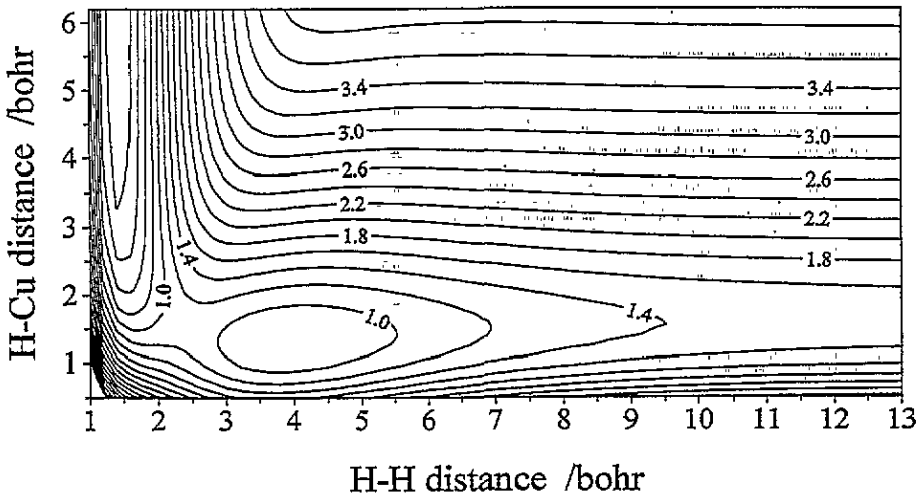

Figure 1. Potential contour diagram for H_2 centre of mass moving perpendicularly to the Cu surface through a threefold site, and H–H bond stretching perpendicular to the surface; energies, in eV, are relative to free H_2, at equilibrium bond distance; the contour interval is 0.2 eV; $\Delta_{HH} = -0.45$, $\Delta_{HCu} = +0.20$.

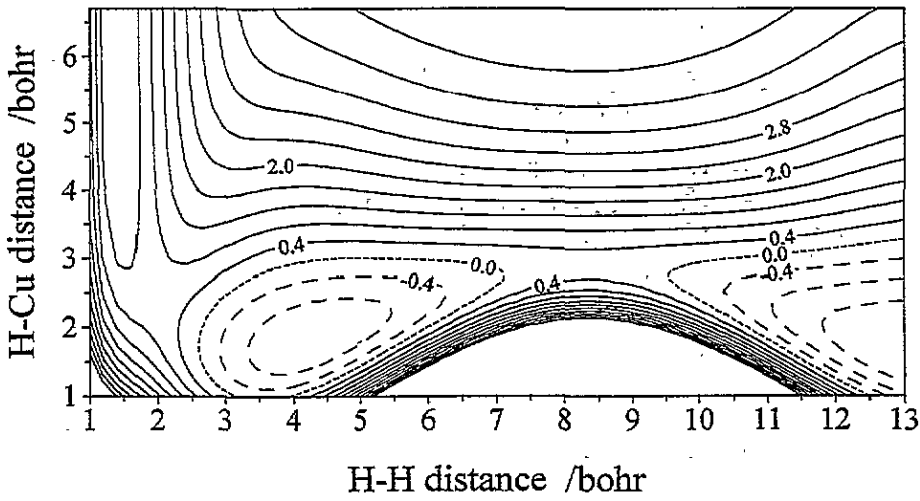

Figure 2. Potential contour diagram for H_2 centre of mass moving perpendicularly to the Cu surface through a bridge site at the centre of the unit cell, and H–H bond stretching parallel to the surface toward on top sites through threefold sites; energies, in eV, are relative to free H_2, at equilibrium bond distance; the contour interval is 0.4 eV; $\Delta_{HH} = -0.45$, $\Delta_{HCu} = +0.20$.

Appropriate values of the Sato parameters, Δ_{HH} and Δ_{HCu}, appearing in the V_{HCu} potential, were selected by examining the equipotential contour diagrams of different two-dimensional approaches of H_2 to Cu(111). We found that when H_2 impinges on the Cu surface with the H–H bond perpendicular to it the chemisorption is energetically much more demanding than when the molecule is parallel to the surface (compare figure 1 to figure 2). For parallel approaches, the H_2–Cu(111) potential shows different features depending on the values of Δ_{HH} and Δ_{HCu}: for positive values of Δ_{HH}, a well of physisorption appears in the entrance channel of the reaction, whereas for negative values, we observed the presence of activation barriers of increasing height for decreasing values of Δ_{HH}. The same trend for the barrier height was observed for the other parameter, Δ_{HCu}, which, on the other hand, influences also the location of the barrier in the reaction path: for increasing positive values, we have barriers closer and closer to the Cu surface, which then become late barriers. For parallel approaches, the heights of the activation barriers can be significantly different at different adsorption sites [27]. Now, experimental measurements generally agree that the dissociative chemisorption of H_2 on Cu surfaces is a highly activated process, with activation energies in the range 0.6 ± 0.4 eV [1, 2, 5, 12, 13, 26], depending on the Cu surface (single crystals, films, foils or powders). Recent experimental studies of the recombinative desorption of D_2 from Cu(111) [13] report an activation barrier of 0.44 eV, and molecular beam experiments [2–7, 10] have shown that both translational and vibrational energy can promote the dissociative adsorption. We varied the Sato parameters in order to have for the most important two-dimensional approaches some of the features coming from experimental data. We found that for $\Delta_{HH} = -0.45$ and $\Delta_{HCu} = +0.20$, which are the values used in our dynamical simulations, the parallel approach with the H_2 centre of mass moving perpendicularly to the Cu surface through the bridge site, and the H–H bond stretching parallel to the line joining adjacent on top sites through threefold sites, has a 'central' barrier of 0.61 eV, as shown in the contour diagram of figure 2 (this value is the difference between the saddle-point energy and potential energy minimum of free H_2). The barrier is located halfway between the entrance and the exit channels, and it corresponds

to a somewhat stretched H_2 molecule ($r_{HH} = 1.99$ Bohr), at a distance $z_{HCu} = 2.40$ Bohr from the surface. For the same values of Δ_{HH} and Δ_{HCu}, other approaches have higher activation barriers. If one considers that the zero- point energy of free H_2 is high (0.27 eV) if compared to the value it can have when H_2 is at the transition state region, we can say that a barrier of 0.61 eV is in good agreement with the mean experimental value. The central position of the barrier in the most favoured two-dimensional approach should lead, at least for that and similar approaches, to a comparable influence of the translational and rovibrational energies on the dissociative adsorption, as found experimentally. We will return to this point when the dynamical results are presented and discussed.

4. Dynamical simulations

The chemisorption dynamics of a H_2 beam on the Cu(111) surface was simulated by using the above-described LEPS potential in a Monte Carlo quasiclassical trajectory treatment [34]. The initial conditions of a trajectory of a diatomic molecule AB colliding with a rigid surface S are completely defined when the values of the following variables are selected: (a) collision kinetic energy of the AB centre of mass, E_{col}; (b) polar and azimuthal angles, Θ and Φ, defining the direction of incidence of AB at the surface; (c) AB vibrational and rotational quantum numbers, v and j; (d) coordinates x_0 and y_0 of the 'aiming point', the ideal point of impact of AB at the surface, in the absence of interaction; (e) polar and azimuthal angles, ϑ and φ, defining the orientation of the A–B bond with respect to the direction of incidence at the surface; (f) rovibrational phase, ξ; (g) orientation of the AB rotational angular momentum, as defined by angle η formed with z axis. The initial distance of the AB centre of mass from the surface was always taken equal to 10 Å, so that, the interaction energy of AB with S was negligible. The beam variables ($E_{col}, \Theta, \Phi, v, j$) defined the 'experimental' conditions of the simulated beam of AB molecules, and the other variables ($x_0, y_0, \vartheta, \varphi, \xi, \eta$) were treated as stochastic variables, and their values selected according to their distribution laws. To reduce the influence of the Monte Carlo statistical fluctuations on the results, we used the same sequence of random numbers for different sets of trajectories, corresponding to different sets of values of the beam variables ($E_{col}, \Theta, \Phi, v, j$).

We analysed the behaviour of the dissociative adsorption probability $P_a(E_{col}, \Theta, \Phi, v, j)$ (initial sticking coefficient), that is, the probability that an incident AB molecule adsorbs on the surface S with bond breaking, when varying the 'experimental' conditions. In our treatment, P_a was approximated by the ratio, N_a/N, between the number of trajectories leading to dissociation (N_a) and adsorption of the AB molecule, and the total number of trajectories (N) computed for selected values of ($E_{col}, \Theta, \Phi, v, j$). For each set of initial conditions, that is, for each set of values of the beam variables ($E_{col}, \Theta, \Phi, v, j$), we computed $N = 2700$ trajectories (N is almost one order of magnitude greater than that used in [23]), so that, the Monte Carlo standard error, $\lambda = [P_a(1 - P_a)/N]^{1/2}$, was at most 0.01. A predictor–corrector method was used to integrate the equations of motion, with a step size of 0.07 fs, which guarantees high accuracy in the numerical integration procedure, with conservation of the total energy of the system during the trajectory up to at least six significant figures.

5. Results and discussion

In simulations of molecule–surface scattering dynamics, it is of particular interest to study how the dissociative adsorption probability, P_a, is influenced by the translational, vibrational

and rotational energy components of the incident molecule.

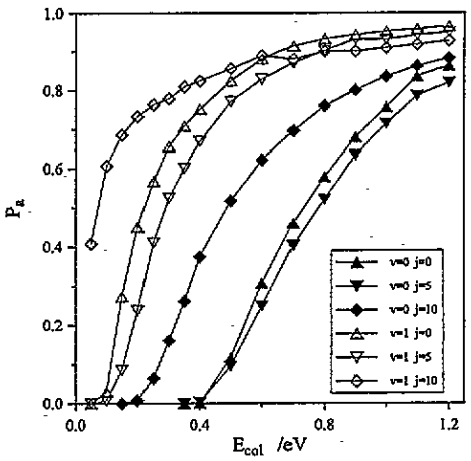

Figure 3. Dissociative adsorption probability against H_2 initial collision energy, for rotational levels $j = 0, 5, 10$, of the two lowest vibrational states; $\Theta = 0°$, $\Phi = 0°$.

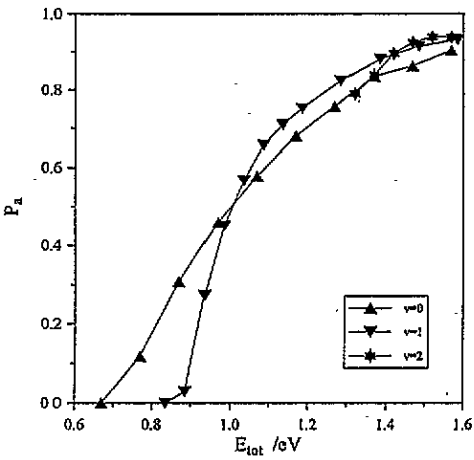

Figure 4. Dissociative adsorption probability against H_2 total energy, for the three lowest vibrational states, $v = 0, 1, 2$; $j = 0$, $\Theta = 0°$, $\Phi = 0°$.

In figure 3, the dependence of P_a on the H_2 initial collision kinetic energy, E_{col}, is shown for different rotational levels ($j = 0, 5, 10$) of the ground ($v = 0$) and first excited ($v = 1$) vibrational state. For $v = 0$ and $j = 0$, we have found a threshold for E_{col} at about 0.4 eV, which means that the chemisorption of H_2 in its ground vibrational state starts at collision energies remarkably lower than the value of the barrier (0.6 eV) given by the LEPS potential for the most favoured approach. This fact is a clear indication that the H_2 molecules use part of the zero-point vibrational energy to cross the barrier of the transition state region, a behaviour in agreement with the diffuse observation that the dissociative adsorption of H_2 on Cu(111) is vibrationally assisted [4, 6, 10, 17]. It is a particularly difficult task to obtain experimental data for the dissociative adsorption probability of H_2 on Cu(111) at E_{col} values above 0.5 eV [2, 4, 5], whereas for D_2 it is possible to reach values of E_{col} just above 0.8 eV [10, 12]. An alternative way to get information about adsorption dynamics is based on the use of the detailed balance principle in studies of time of flight distributions of molecules desorbed from the surface [14], which allow regions of higher values of E_{col} to be explored, and data for quantum state specific dynamics to be obtained. Adsorption and desorption experiments indicate that the chemisorption of D_2 molecules in the $v = 0$, $j = 0$ state starts at about 0.35 eV of collision energy, in agreement with our results for H_2, and reaches the saturation level at $E_{col} = 0.9$ eV along an S-shaped curve which is steeper than the theoretical curve obtained from our simulations. From an analysis of the two sets of curves in figure 3 corresponding to the vibrational states $v = 0$ and $v = 1$, it comes out that the adsorption probability P_a depends critically on the vibrational energy of H_2, the $v = 1$ curves being shifted to E_{col} values much lower than those with $v = 0$. The chemisorption threshold of H_2 molecules in their first excited vibrational state is at $E_{col} = 0.05$ eV, and the sticking coefficient P_a increases toward the saturation value 0.9 along curves steeper than those corresponding to $v = 0$, thus showing a trend similar to that observed experimentally for D_2 [14]. The shift of the $v = 1$, $j = 0$ curve with respect to the $v = 0$, $j = 0$ curve is

smaller for low than for high values of P_a, the distance between the two curves increasing from 0.35 eV at $P_a = 0$ to 0.60 eV at the saturation value $P_a = 0.9$ (the energy difference between the $v = 1$ and $v = 0$ states is 0.516 eV).

The relative importance of the role played by the vibrational against the translational energy components of the incident beam in dissociative adsorption can be evidenced by a study of the dependence of P_a on the H_2 total energy, $E_{tot} = E_{vib} + E_{col}$, as shown in figure 4. At E_{tot} values above 1.3 eV, the curves obtained for states $v = 0$, $v = 1$ and $v = 2$ are nearly superimposed. The same is true for curves $v = 0$ and $v = 1$ in the range 1.0 to 1.3 eV, even if the curve $v = 1$ is slightly higher than that for $v = 0$. In this range of energies, the adsorption mechanism is almost exclusively controlled by the total energy, independently of its partitioning in translational and vibrational contributions, even if the vibration seems to play a somewhat prominent role if compared to the translation. For $E_{tot} < 1.0$ eV, the $v = 0$ and $v = 1$ curves have different behaviours, because the $v = 1$ curve goes to zero more rapidly than the $v = 0$ curve, that is, in this range the vibrational energy is significantly less important than the collisional one in promoting dissociative chemisorption. The effectiveness of the vibrational energy can be better defined by making use of the vibrational efficacy, ε_v, as given [14] by the ratio between the difference of the E_{col} values corresponding to the same P_a value for the vibrational states $v = 0$ and $v = 1$, and the difference between the energies of those two states (0.516 eV). From our data, it comes out that ε_v is 0.68 at the threshold values $P_a = 0$ (that is, vibration is less effective than translation in this range of collision energies), it increases to 1.0 at $P_a = 0.5$ and rises to 1.2 at saturation value $P_a = 0.9$ (vibration more effective than translation). A theoretical study [20] on the influence of the potential topologies on P_a using a quantum wave packet approach has pointed out that high efficacy of the vibrational energy in promoting adsorption should be typical of late barrier potentials. In our case, we have found that the vibration is effective on the whole range of E_{col}, and even near the thresholds it is appreciably higher (0.68) than the value (0.20) found in [18] for a central barrier potential, but it is comparable to the value (0.56) obtained for a late barrier. Our results are unexpected on the basis of a classification scheme [41] which assigns to central barriers behaviours intermediate between those of early and late barriers, and this could be in part due to the increased complexity of the dynamical problem when the full dimensionality of the potential hypersurface is taken into account, as in our calculations.

The role of the rotational energy of the incident beam can be understood by looking at curves in figures 3 and 5. When H_2 is allowed to rotate in low rotational states ($j < 5$), we observe a decrease of the chemisorption probability P_a, followed by an increase for values of j greater than four, that is, rotation first inhibits and then enhances dissociation. The initial decrease of P_a with increasing j at low j values is due to the strong influence of the orientation of H_2 on the potential energy surface, as shown above when describing the features of the potential. If the molecule rotates, the probability of reaching the transition state region in a geometry favourable to dissociation decreases, but, if the value of j is sufficiently high, then there is a transfer of energy from rotation into translation along the reaction path, which arises from the stretching of the bond at the transition state. So, it comes out that at low j values a steric effect tends to inhibit dissociation, whereas at high j values an energy effect enhancing dissociation becomes predominant. This is true for H_2 molecules both in their ground and first excited vibrational states (the curve $j = 5$ in figure 3 shift to the right, both for $v = 0$ and $v = 1$). The same trend has been found in recent experimental work on the D_2–Cu(111) system [9, 14], which has shown, on the basis of detailed balance arguments, that the rotational excitation of D_2 increases the adsorption threshold and therefore decreases P_a at low j values ($j < 5$), with a reversal of

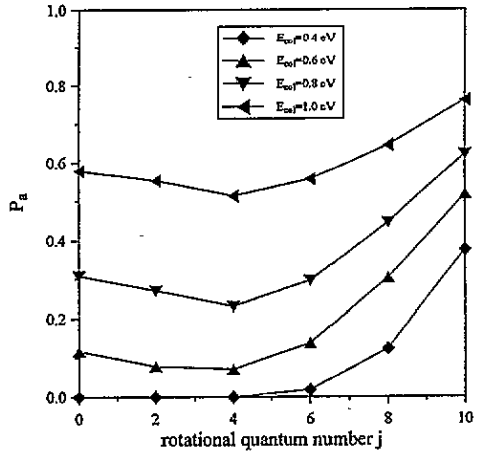

Figure 5. Dissociative adsorption probability against rotational quantum number, j, for different initial collision energies, E_{col}; $v = 0$, $\Theta = 0°$, $\Phi = 0°$.

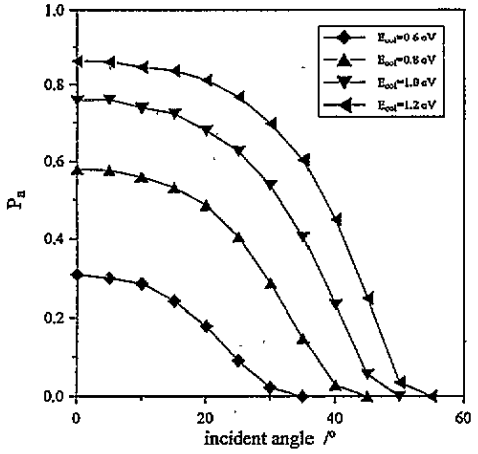

Figure 6. Dissociative adsorption probability against incident polar angle, Θ, for different initial collision energies, E_{col}; $v = 0$, $j = 0$, $\Phi = 0°$.

the trend at high j values. Theoretical calculations [23], based on a quantum mechanical wave packet approach, with a late barrier potential (in the exit channel), a position rather different from the central one of our most favoured approaches, have shown the same kind of behaviour. Finally, we can observe in figure 5 that at the threshold value of the initial collision energy (0.4 eV), the sticking probability P_a increases monotonically with j, as found in recent quantum dynamical calculations [22]. Results similar to those presented here for the influence of vibrational and rotational energies have been found in full-dimensional quantum-classical calculations for the chemisorption of H_2 on Cu(110) [24] and in classical calculations for the system H_2–Ni(001) [42].

We studied the dependence of P_a on the incident angle, Θ, of the H_2 beam at the metal surface, for different values of the initial collision energy, and the results are shown in figure 6. We can see that P_a decreases rapidly for increasing values of Θ, and the slope is different for different values of E_{col}. Now, it is convenient [2, 4] to represent the dependence of P_a on Θ with the value of the exponent n in the expression relating P_a at Θ to its value at $0°$: $P_a(\Theta)\cos(\Theta)/P_a(0°) = \cos^n(\Theta)$. In our case, we have found for n the values 12.2, 6.3, 4.6 and 3.6 for $E_{col} = 0.6$, 0.8, 1.0, 1.2 eV, respectively. As observed experimentally [2, 4], the exponent n is high at low values of E_{col}, and decreases when E_{col} increases, that is, the ratio $P_a(\Theta)/P_a(0°)$ decreases with Θ more rapidly at low than at high collision energies. In figure 7, we report P_a against Θ for different values of the normal component of translational energy, $E_n = E_{col}\cos^2\Theta$. It is evident that for sufficiently high values of E_n (>0.6 eV), P_a is practically independent of Θ, that is, the sticking probability scales with normal energy component, as found in molecular beam experiments [2, 4].

We have also investigated whether there is in our potential an azimuthal anisotropy of P_a. This study was done by varying the azimuthal angle, Φ, of approach of H_2 to the Cu surface at four different values of E_{col}: 0.6, 0.8, 1.0, 1.2 eV. We have seen that the curves P_a/Θ obtained for $\Phi = 15°, 30°, 45°$ are practically coincident with those found for $\Phi = 0°$, the observed variations being well below the Monte Carlo standard errors.

It is interesting to analyse the translational, vibrational and rotational energy distributions

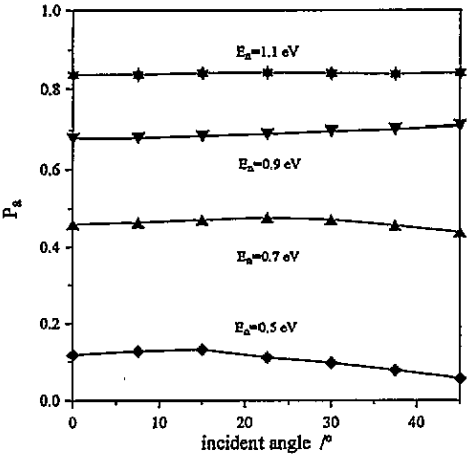

Figure 7. Dissociative adsorption probability against incident polar angle of H_2, Θ, for different normal collision energies, E_n, $v = 0$, $j = 0$, $\Phi = 0°$.

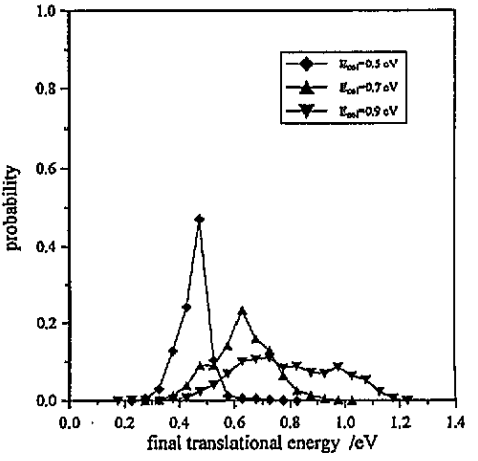

Figure 8. Translational energy distributions of scattered H_2 molecules for different initial collision energies, E_{col}; $v = 0$, $j = 0$, $\Theta = 0°$, $\Phi = 0°$; the bin width is 50 meV.

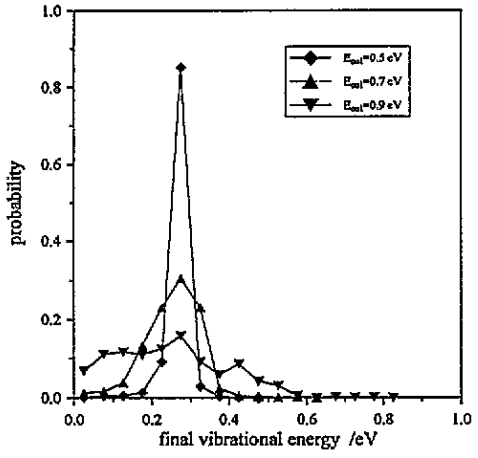

Figure 9. Vibrational energy distributions of scattered H_2 molecules for different initial collision energies, E_{col}; $v = 0$, $j = 0$, $\Theta = 0°$, $\Phi = 0°$; the initial vibrational energy is 269 meV; the bin width is 50 meV.

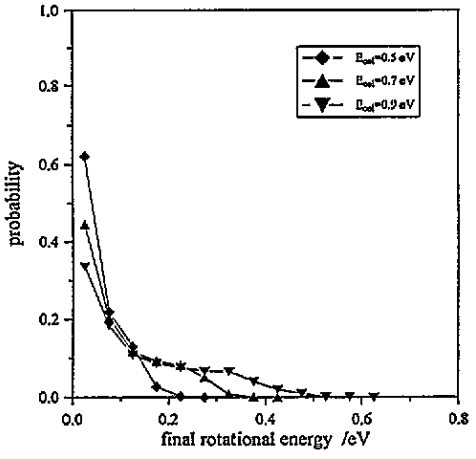

Figure 10. Rotational energy distributions of scattered H_2 molecules for different initial collision energies, E_{col}; $v = 0$, $j = 0$, $\Theta = 0°$, $\Phi = 0°$; the bin width is 50 meV.

of the scattered H_2 molecules to find out at what extent the energy is converted, along the reaction path, from one degree of freedom to another. The results of this analysis are shown in figures 8, 9 and 10, for three different values of initial collision energy: $E_{col} = 0.5$, 0.7, 0.9 eV, and for a beam normal to the surface ($\Theta = \Phi = 0°$), with molecules in their ground rovibrational state ($v = j = 0$). In the case $E_{col} = 0.5$ eV, just above the translational threshold, 87% of molecules are scattered with increase of internal energy at the expense of their translational energy, and 85% of them have vibrational energy

which differs from its initial value by less than 10%. At higher incident energies, the percentage of molecules with translational energy lower than E_{col} decreases to 76% and 70% at $E_{col} = 0.7$ and 0.9 eV whereas only 31% and 16% of molecules do not change their initial vibrational state. The average final vibrational energy of scattered molecules is lower than its initial value by 4, 14 and 25 meV for $E_{col} = 0.5$, 0.7 and 0.9 eV, respectively. Keeping in mind that in quasiclassical calculations the H_2 internal energy is quantized only at the beginning of each trajectory, we can say that the vibrational temperature of the beam remains practically constant for increasing values of E_{col}. Correspondingly, the non-adsorbed molecules, which do not rotate at the beginning of the trajectories, undergo an increase of their average rotational energy equal to 50, 90 and 137 meV, for the considered values of E_{col}, and for $E_{col} = 0.9$ eV rotational levels up to $j = 10$ are populated. This significant coupling of translational to rotational motion, which is increasingly important for increasing values of E_{col}, accompanied by the absence of energy transfer to the vibrational degree of freedom, is responsible for the fact that molecules are inelastically scattered instead of being chemisorbed.

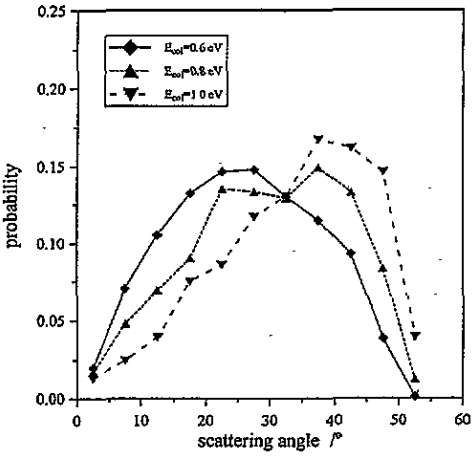

Figure 11. Angular distributions of scattered H_2 molecules for different initial collision energies, E_{col}, at incident angle $\Theta = 25°$; $v = 0$, $j = 0$, $\Phi = 0°$; the bin width is 5°.

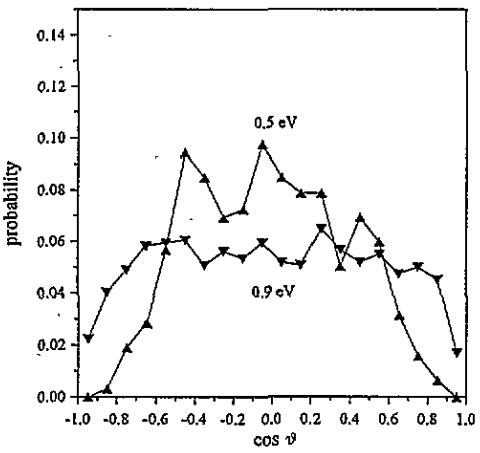

Figure 12. Cumulative distribution function of the polar angle, ϑ, defining the initial orientation of the molecular axis for adsorbed H_2 molecules, at initial collision energies, $E_{col} = 0.5$ and 0.9 eV; $v = 0$, $j = 0$, $\Theta = 0°$, $\Phi = 0°$.

The angular distributions of the scattered H_2 molecules are shown in figure 11 for different values of E_{col}, at incident angle $\Theta = 25°$. It comes out that, at $E_{col} = 0.6$ eV, the angular distribution is symmetric with respect to the incident angle $\Theta = 25°$ (53% of molecules are scattered at angles greater than 25°), that is, the scattering is nearly at specular angle. This feature, together with negligible changes in vibrational energy, is an indication that these molecules do not sample the dissociative part of the interaction potential, where the H–H bond is stretched. When E_{col} is increased to 0.8 and 1.0 eV, the distribution curves are more asymmetric, and the scattering becomes progressively supraspecular, with a percentage of molecules scattered at polar angles greater than 25° equal to 64% and 76%, respectively.

Finally, in figure 12, we have drawn the cumulative distribution function ($\cos\vartheta$) of the polar angle, ϑ, defining the orientation of the molecular axis with respect to the incident

direction of the beam, for adsorbed H_2 molecules, at $E_{col} = 0.5$ and 0.9 eV. For the whole set of trajectories leading to adsorption or scattering, the $\cos\vartheta$ function is uniformly distributed in the range -1 to $+1$, but it may be immediately observed that, at $E_{col} = 0.5$ eV, the fraction of chemisorbed molecules with H–H bond axis initially oriented at $\vartheta < 50°$ (or equivalently, $\vartheta > 130°$) is rather low, that is, about 5%. If one considers that, for this value of E_{col}, the rotational excitation of the backscattered molecules is negligible, it is possible to say that the fact that chemisorption is preferentially observed for initial orientations of the molecular axis parallel to the Cu surface is due to the larger potential barriers encountered by H_2 in perpendicular rather than in parallel approaches (compare figure 1 to figure 2). When E_{col} is increased well above its threshold value, this orientation effect on the sticking probability gradually disappears (see figure 12, curve at $E_{col} = 0.9$ eV), because the excess of translational energy is used in overcoming the adsorption barrier even if the molecular bond orientation is not favourable.

To determine the possible consequences on dynamical results due to the introduction of non-local corrections in our band structure calculations, we performed a few simulations with values of the H–Cu(111) binding energies 20% lower than those in table 1 (20% is the estimated H–Cu overbinding due to the absence of non-local corrections). Using the same values of the Sato parameters as used throughout all calculations ($\Delta_{HH} = -0.45$, $\Delta_{HCu} = +0.20$), we found that a beam with $\Theta = \Phi = 0°$ and $v = j = 0$ has an E_{col} threshold located at 1.0 eV, that is, at a value remarkably higher than that of curve $v = 0$ of figure 3. For higher values of Δ_{HH}, the E_{col} threshold decreases, and it is located at 0.2 eV for $\Delta_{HH} = -0.20$. In any case, the trend of P_a against E_{col} is similar to that of curve $v = 0$ in figure 3, obtained using the *ab initio* values of D_{HCu} without non-local corrections.

It is worthwhile to make a comment on the rigid-surface constraint. Recent theoretical investigations [25], based on joint use of classical mechanics and wave packet methods, have shown that the average energy transferred from H_2 to surface phonons is typically 7-8% of the impact energy, a value comparable to 6% given by the hard-sphere approximation. Moreover, it is generally accepted [14] that the adsorption of H_2 on the Cu surface occurs in a single collision, and this should greatly reduce the consequences of the rigid-surface approximation on the chemisorption probability.

6. Conclusions

A LEPS potential for H_2 interacting with the Cu(111) surface was built starting from *ab initio* density functional results for atomic hydrogen adsorbed on the Cu surface, and used in quasiclassical trajectory simulations. We investigated the influence of the different components of the total energy of H_2 on the dissociative adsorption probability, and we found that both the collisional and vibrational energies can be effective in promoting dissociative chemisorption. For high values of H_2 total energy, translation and vibration play an almost equivalent role, even if vibration appears to be a little more effective than is translation in promoting dissociative adsorption. For low values of H_2 total energy, the role of the translational component is prevalent with respect to the vibrational one. The rotational motion of H_2 has two effects on chemisorption, a steric effect at low j values which inhibits the dissociation of the H–H bond, and an energy effect at high j values which enhances it. The dependence of P_a on the angle of incidence of the hydrogen beam at the Cu surface follows the normal energy scaling only for higher initial collision energies. No azimuthal corrugation of the potential used in our calculations is observed.

Acknowledgments

This work was supported by Ministero dell'Università e della Ricerca Scientifica e Tecnologica, and by Consiglio Nazionale delle Ricerche. Some of the simulations were performed on the Convex-HP-META cluster system of Consorzio Interuniversitario Lombardo di Elaborazione Automatica as a project of Centro di Modellistica Computazionale.

References

[1] Kubiak G D, Sitz G O and Zare R N 1985 *J. Chem. Phys.* **83** 2538
[2] Anger G, Winkler A and Rendulic K D 1989 *Surf. Sci.* **220** 1
[3] Hayden B E and Lamont C L A 1989 *Phys. Rev. Lett.* **63** 1823
[4] Berger H F, Leisch M, Winkler A and Rendulic K D 1990 *Chem. Phys. Lett.* **175** 425
[5] Hayden B E and Lamont C L A 1991 *Surf. Sci.* **243** 31
[6] Hodgson A, Moryl J and Zhao H 1991 *Chem. Phys. Lett.* **182** 152
[7] Hayden B E 1991 *Dynamics of Gas–Surface Interactions* ed C T Rettner and M N R Ashfold (London: Royal Society of Chemistry)
[8] Rettner C T, Michelsen H A, Auerbach D J and Mullins C B 1991 *J. Chem. Phys.* **94** 7499
[9] Michelsen H A, Rettner C T and Auerbach D J 1992 *Phys. Rev. Lett.* **69** 2678
[10] Rettner C T, Auerbach D J and Michelsen H A 1992 *Phys. Rev. Lett.* **68** 116
[11] Michelsen H A, Rettner C T and Auerbach D J 1992 *Surf. Sci.* **272** 65
[12] Auerbach D J, Rettner C T and Michelsen H A 1993 *Surf. Sci.* **283** 1
[13] Rettner C T, Michelsen H A and Auerbach D J 1993 *Faraday Discuss. Chem. Soc.* **96** 1731
[14] Michelsen H A, Rettner C T, Auerbach D J and Zare R N 1993 *J. Chem. Phys.* **98** 8294
[15] Harris J and Andersson S 1985 *Phys. Rev. Lett.* **55** 1583
[16] Harris J, Holloway S, Rahman T S and Yang K 1988 *J. Chem. Phys.* **89** 4427
[17] Hand M R and Holloway S 1989 *J. Chem. Phys.* **91** 7209
[18] Harris J 1989 *Surf. Sci.* **221** 335
[19] Nørskov J K 1989 *J. Chem. Phys.* **90** 7461
[20] Halstead D and Holloway S 1990 *J. Chem. Phys.* **93** 2859
[21] Kuchenhoff S, Brenig W and Chiba Y 1991 *Surf. Sci.* **245** 389
[22] Dai J, Sheng J and Zhang J Z H 1994 *J. Chem. Phys.* **101** 1555
[23] Darling G R and Holloway S 1993 *Faraday Discuss. Chem. Soc.* **96** 43; 1994 *J. Chem. Phys.* **101** 3268; 1994 *Surf. Sci.* **321** L189
[24] Kumar S and Jackson B 1994 *J. Chem. Phys.* **100** 5956
[25] Billing G D and Cacciatore M 1993 *Faraday Discuss. Chem. Soc.* **96** 33
[26] Michelsen H A, Rettner C T and Auerbach D J 1994 *Surface Reactions* ed R J Madix (Berlin: Springer)
[27] Forni A, Wiesenekker G, Baerends E J and Tantardini G F 1994 *Int. J. Quantum Chem.* **52** 1067
[28] Velde G and Baerends E J 1991 *Phys. Rev.* B **44** 7888
[29] Folga E and Ziegler T 1993 *J. Am. Chem. Soc.* **115** 5169
[30] Velde G and Baerends E J 1993 *Chem. Phys.* **177** 399
[31] Hammer B, Jacobsen K W and Nørskov J K 1993 *Phys. Rev. Lett.* **70** 3971
[32] Becke A D 1988 *Phys. Rev.* A **38** 3098
[33] Perdew J P 1986 *Phys. Rev.* B **33** 8822
[34] Tantardini G F and Simonetta M 1981 *Surf. Sci.* **105** 577
[35] Tantardini G F and Simonetta M 1982 *Chem. Phys. Lett.* **87** 420
[36] Cremaschi P, Tantardini G F, Muilu J and Pakkanen T A 1990 *Vacuum* **41** 260
[37] Forni A and Tantardini G F 1991 *J. Chem. Soc. Faraday Trans.* **87** 447
[38] Tantardini G F 1992 *Cluster Models for Surface and Bulk Phenomena (ASI series B283)* ed G Pacchioni, P S Bagus and F Parmigiani (New York: Plenum)
[39] Bourcet A and Tantardini G F 1994 *J. Electron Spectrosc. Relat. Phenom.* **69** 55
[40] Goodman F O and Wachman H Y 1967 *J. Chem. Phys.* **46** 2376
[41] Polanyi J C 1972 *Accounts Chem. Res.* **5** 161
[42] Beauregard J N and Mayne H R 1994 *Chem. Phys. Lett.* **205** 515